Supporting Information

Rational Design of Cobaltocenium-containing Polythioether Type Metallo-polyelectrolyte as HCl Corrosion Inhibitor for Mild Steel

Shuang Liu[a,b,‡], Jing Yan[a,b,‡], Junqin Shi[c], Xuezhuang Li[a,b], Junping Zhang[b], Xuanyi Wang[b], Ningjing Cai[d], Quanhai Fang[b], Qiuyu Zhang[b], Yi Yan[a,b,]*

[a]Chongqing Technology Innovation Center, Northwestern Polytechnical University, Chongqing, 401135, P. R. China

[b]Department of Chemistry, School of Chemistry and Chemical Engineering, Key Laboratory of Special Functional and Smart Polymer Materials of Ministry of Industry and Information Technology, Northwestern Polytechnical University, Xi'an, 710129, P. R. China

[c]State Key Laboratory of Solidification Processing, Center of Advanced Lubrication and Seal Materials, School of Materials Science and Engineering, Northwestern Polytechnical University, Xi'an, 710072, P. R. China

[d]Queen Mary University of London Engineering School, Northwestern Polytechnical University, Xi'an, 710072, P. R. China

[‡]These authors contributed equally to this work.

Corresponding author: yanyi@nwpu.edu.cn

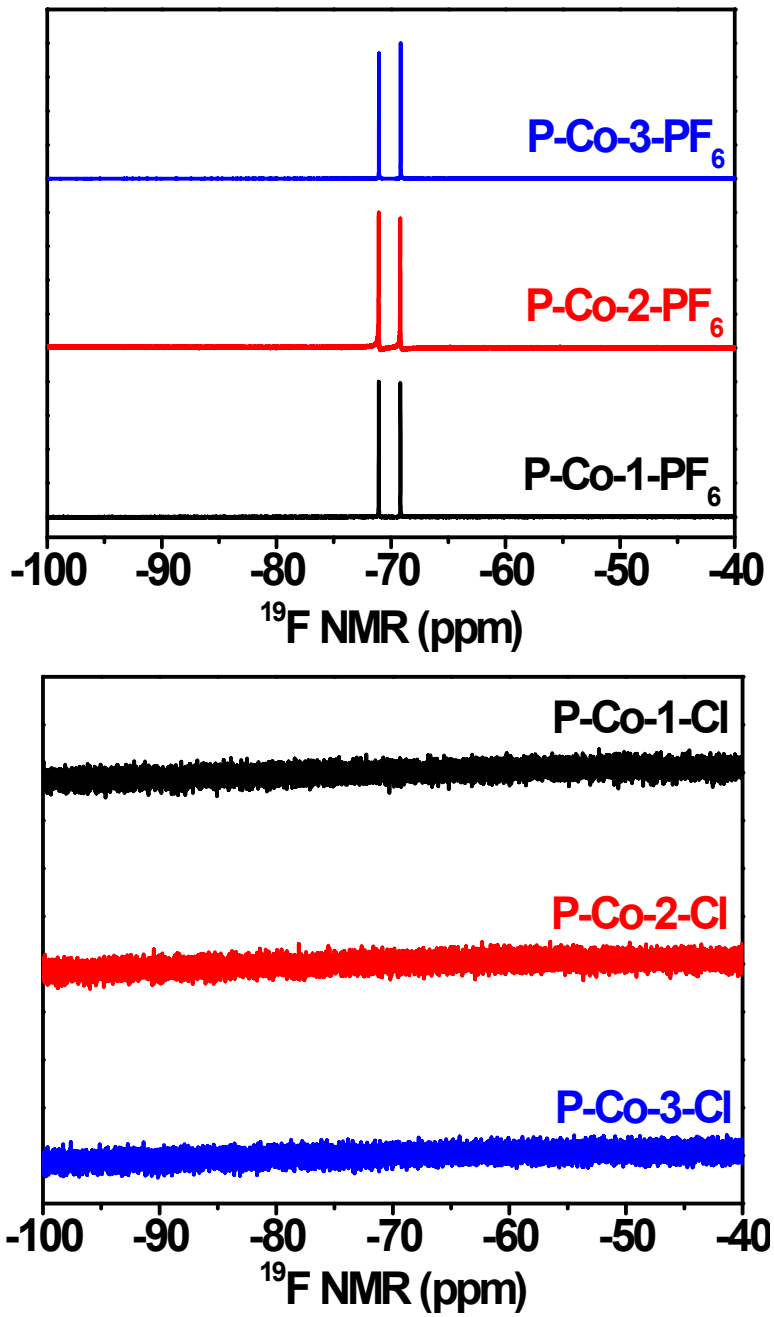

Figure S1. ^{19}F NMR spectra of resulted inhibitors before (top) and after (bottom) counterion exchange.

Figure S2. Photos of the resulted inhibitors: **P-Co-1-PF$_6$**, **P-Co-2-PF$_6$**, **P-Co-3-PF$_6$** (from left to right).

Figure S3. Photos of the resulted inhibitor in D_2O: **P-Co-1-PF$_6$**, **P-Co-2-PF$_6$**, **P-Co-3-PF$_6$** (from left to right).

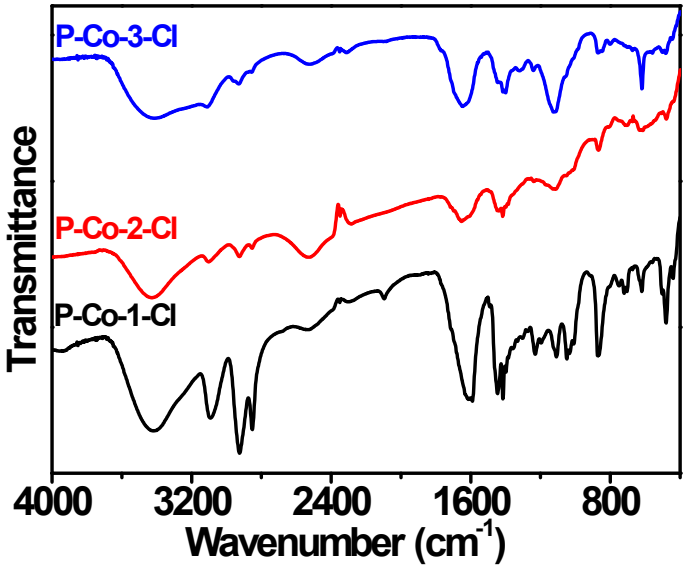

Figure S4. FT-IR spectra of resulted inhibitors.

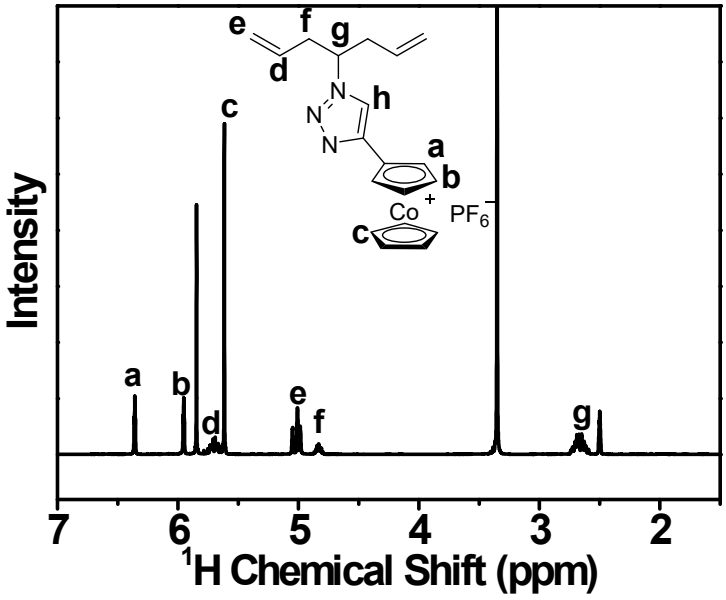

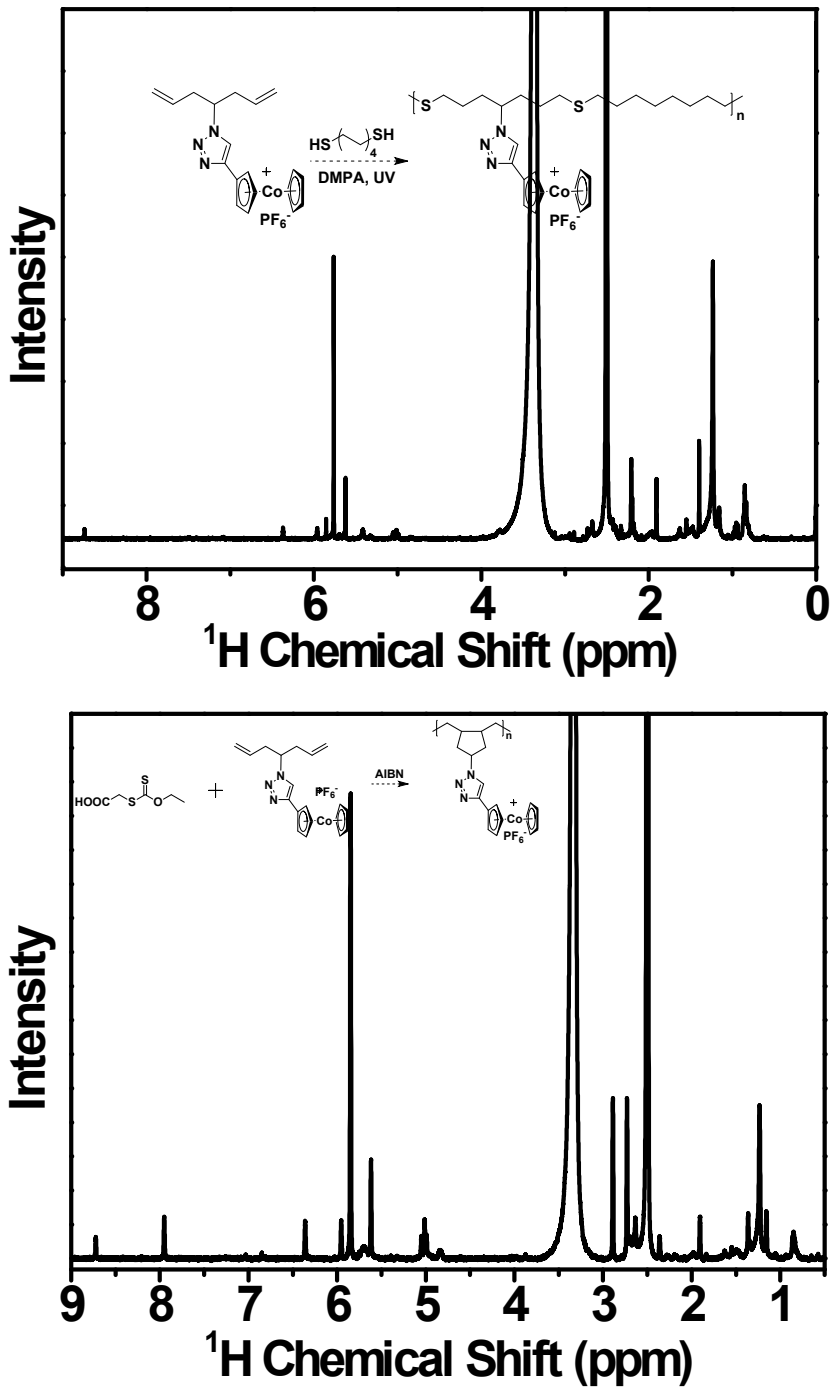

Figure S5. ^{1}H NMR spectra in d_6-DMSO for cobaltocenium-based diene monomer (top), crude after photo-induced thiol-ene polymerization (middle), crude after RAFT/MADIX polymerization (bottom).

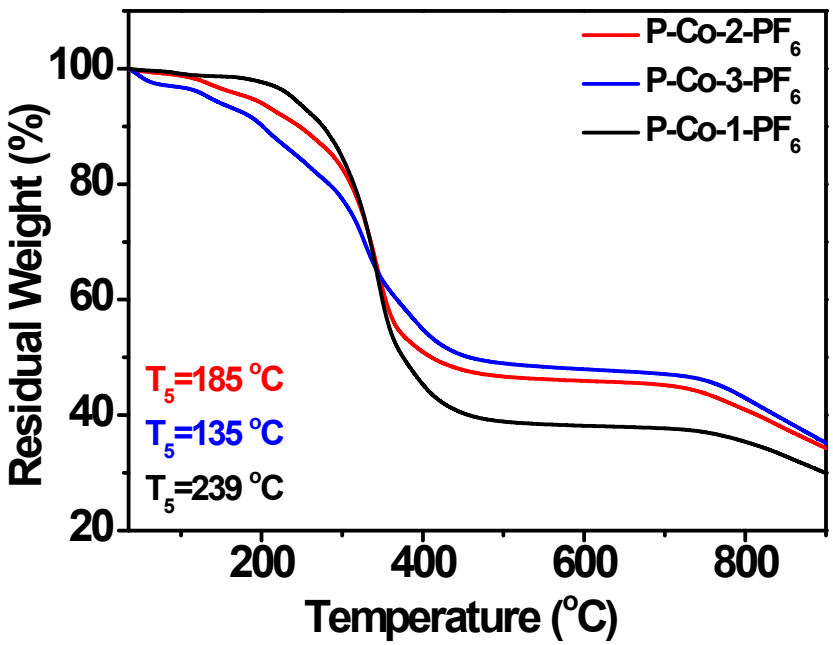

Figure S6. TGA curves of three cobaltocenium-containing polythioethers.

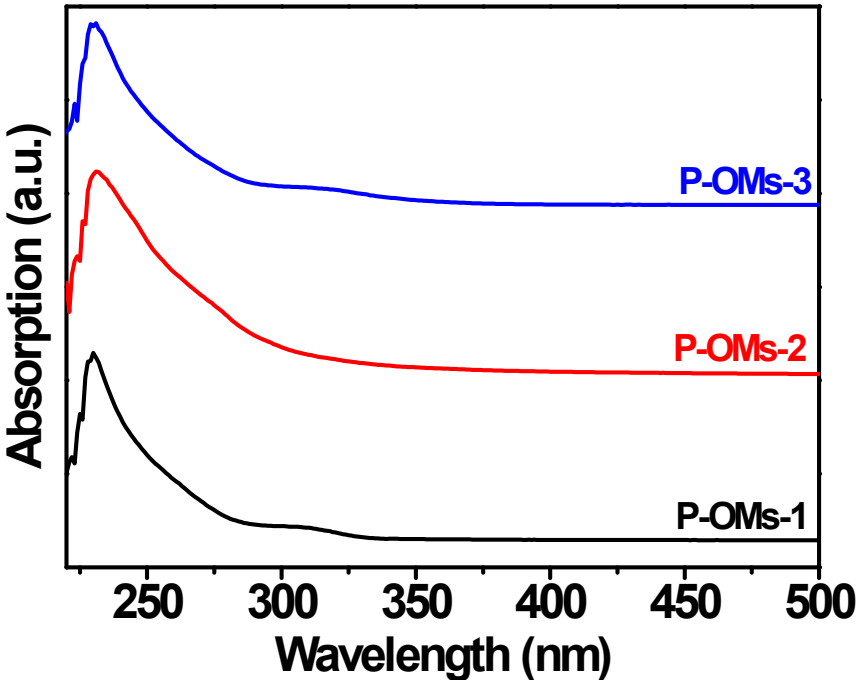

Figure S7. UV-visible spectra of precursor polythioethers.

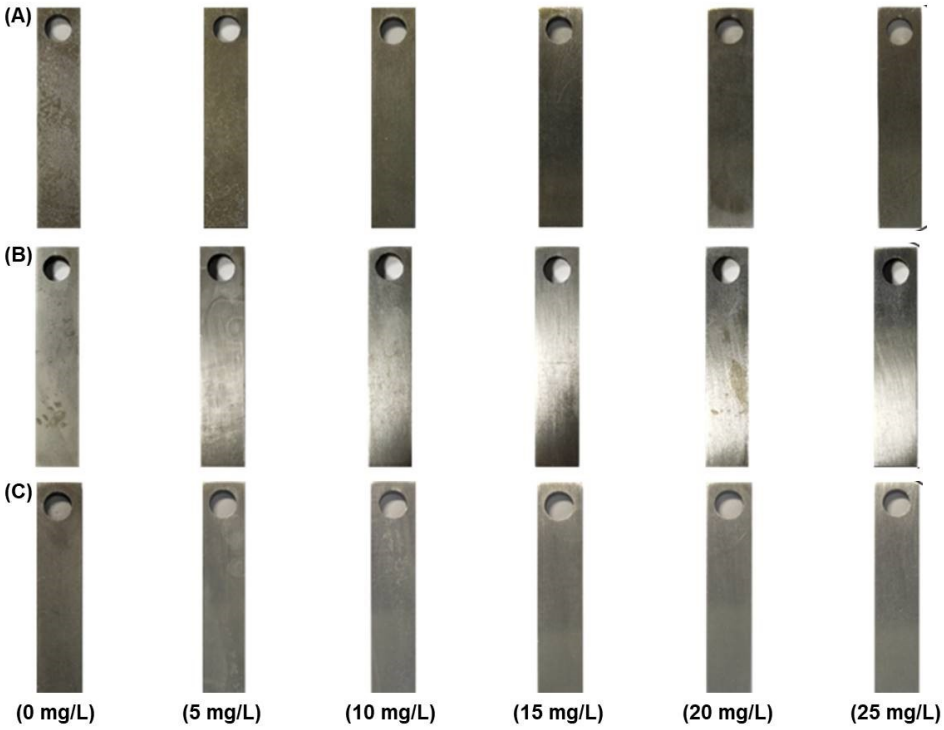

Figure S8. Optical images of steel immersed in corrosion systems with corrosion inhibitors and without inhibitors at different concentration of inhibitors for 2 h. (A: **P-Co-1-Cl**; B: **P-Co-2-Cl**; C: **P-Co-3-Cl**)

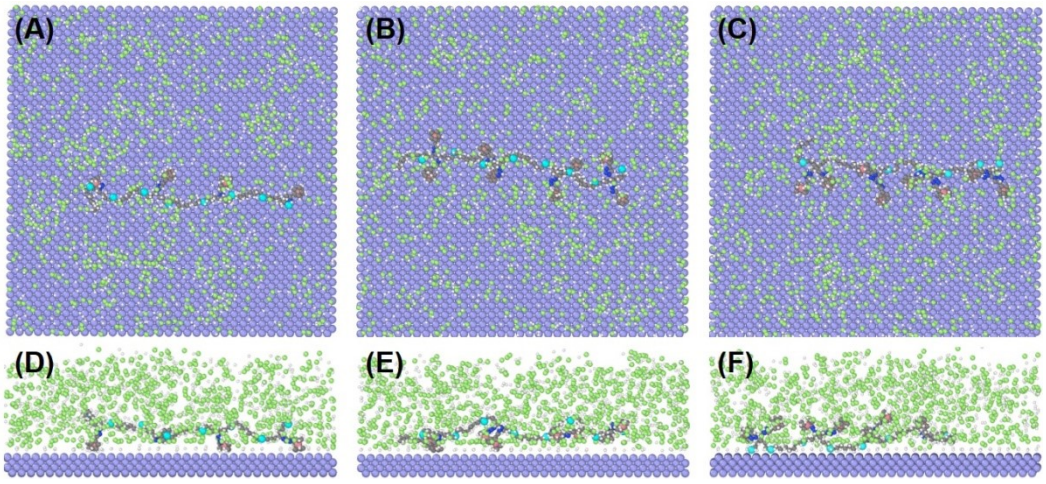

Figure S9. The optimized configuration for the inhibitors **P-Co-1-Cl**, **P-Co-2-Cl**, **P-Co-3-Cl** with four repeat units adsorbed on Fe (110) in the presence of H_2O obtained from molecular dynamic simulation: (**A**)-(**C**) top view; (**D**)-(**E**) side view. (● Cl, ○ H+, ● S, ● N, ● Co).

Table S1. The molecular weight of methylsulfonate-containing polythioether.

Samples	M_n (g/mol)	Đ
P-OMs-1	6900	1.63
P-OMs-2	8900	1.60
P-OMs-3	6600	1.46

Table S2. Electrochemical parameters from the potentiodynamic polarization measurements for mild steel in 5 wt% HCl with different concentration of **P-Co-2-Cl** at 25 °C.

C (mg/L)	E_{corr} (mV)	I_{corr} (μA·cm^{-2})	$-b_c$ (mV·dec^{-1})	b_a (mV·dec^{-1})	η(%)
0	−460.5	82.73	82.00	94.80	/
5	−486.2	20.36	44.15	78.16	75.39
10	−494.9	17.75	95.46	59.35	78.55
15	−505.4	16.17	72.17	50.07	80.46
20	−525.0	14.36	103.55	34.58	82.64
25	-519.9	11.86	69.01	51.71	85.67

Table S3. Electrochemical parameters from the potentiodynamic polarization measurements for mild steel in 5 wt% HCl with different concentration of **P-Co-3-Cl** at 25 °C.

C (mg/L)	E_{corr} (mV)	I_{corr} (μA·cm^{-2})	$-b_c$ (mV·dec^{-1})	b_a (mV·dec^{-1})	η (%)
0	−460.5	82.73	82.00	94.80	/
5	−503.8	19.43	79.90	46.92	76.52
10	−503.1	16.84	52.64	67.43	79.65
15	−519.3	14.19	64.40	54.64	82.85
20	−536.8	10.88	62.90	55.77	86.85
25	−543.8	9.65	143.32	27.22	88.34

Table S4. Electrochemical parameters from the EIS measurements for mild steel in 5 wt% HCl with different concentration of **P-Co-1-Cl** at 25 °C.

C (mg/L)	Rs (Ω·cm^2)	Y_0	n	C_{dl} (μF·cm^{-2})	R_{ct} (Ω·cm^2)	f_{max}	η(%)
0	0.6141	2.037×10^{-5}	0.8927	32.65	121.3	12.4	/
5	0.6363	5.909×10^{-5}	1	59.09	499.8	7.97	75.7
10	0.3050	4.460×10^{-5}	1	44.60	547.9	8.94	77.9
15	0.3259	8.457×10^{-5}	1	84.57	665.9	6.35	81.8
20	0.2476	4.037×10^{-5}	1	40.37	800.9	7.97	84.9
25	0.2513	1.778×10^{-5}	1	17.78	557.1	5.66	78.2

Table S5. Electrochemical parameters from the EIS measurements for mild steel in 5 wt% HCl with different concentration of **P-Co-2-Cl** at 25 °C.

C (mg/L)	*Rs* (Ω·cm^2)	Y_0 ($W^{-1}cm^{-2}$)	n	C_{dl} (μF cm^{-2})	R_{ct} (Ω·cm^2)	f_{max}	η(%)
0	0.6141	2.037×10^{-5}	0.8927	32.65	121.3	12.4	/
5	0.1167	4.009×10^{-5}	1	40.09	461.7	5.66	73.7
10	0.1557	7.431×10^{-4}	1	74.31	600.3	4.97	79.8
15	0.1141	6.449×10^{-5}	1	64.49	655.0	3.94	81.5
20	0.1558	6.122×10^{-4}	1	61.22	806.0	3.94	85.0
25	0.1507	4.999×10^{-4}	1	49.99	918.9	4.97	86.8

Table S6. Electrochemical parameters from the EIS measurements for mild steel in 5 wt% HCl with different concentration of **P-Co-3-Cl** at 25 °C.

C (mg/L)	*Rs* (Ω·cm^2)	Y_0	*n*	C_{dl} (μF·cm^{-2})	R_{ct} (Ω·cm^2)	f_{max}	η(%)
0	0.6141	2.037×10^{-5}	0.8927	32.65	121.3	12.4	/
5	0.1991	1.443×10^{-5}	1	14.43	820.8	7.97	85.2
10	0.1935	1.847×10^{-5}	1	18.47	1028	6.35	88.2
15	0.1657	1.742×10^{-5}	1	17.42	1429	5.66	91.5
20	0.1981	1.310×10^{-5}	1	13.10	961.2	6.35	87.4
25	0.1793	1.668×10^{-5}	1	16.68	918.4	6.35	86.8

Table S7. The elemental composition for mild steel.

Element	C	Si	Mn	P	S	Cr	Zn	Mo	Al	Cu	Ti	Fe
Content (%)	0.08	0.18	0.45	0.03	0.03	0.12	0.0003	0.001	0.01	0.25	0.25	98.60